



HAL
open science

Classification of 3D objects by random extraction of discriminant sub-parts for the study of the sub-soil in oil prospecting

François Meunier, Christophe Marsala, Laurent Castanie

► To cite this version:

François Meunier, Christophe Marsala, Laurent Castanie. Classification of 3D objects by random extraction of discriminant sub-parts for the study of the sub-soil in oil prospecting. *Advances in Knowledge Discovery and Management*, In press. hal-01694012

HAL Id: hal-01694012

<https://hal.sorbonne-universite.fr/hal-01694012v1>

Submitted on 26 Jan 2018

HAL is a multi-disciplinary open access archive for the deposit and dissemination of scientific research documents, whether they are published or not. The documents may come from teaching and research institutions in France or abroad, or from public or private research centers.

L'archive ouverte pluridisciplinaire **HAL**, est destinée au dépôt et à la diffusion de documents scientifiques de niveau recherche, publiés ou non, émanant des établissements d'enseignement et de recherche français ou étrangers, des laboratoires publics ou privés.

Classification of 3D objects by random extraction of discriminant sub-parts for the study of the sub-soil in oil prospecting

Francois Meunier, Christophe Marsala and Laurent Castanie

Abstract In this paper, we propose a new approach for the classification of 3D objects inspired by the *Time Series Shapelets* of [Ye and Keogh, 2009].

The idea is to use discriminating sub-surfaces for the current classification in order to take into account the local nature of the relevant elements. This allows the user to have knowledge concerning the sub-parts that have been useful for determining the belonging of an object to a class, and to get a better classification rate than current state of the art methods.

The results obtained confirm the advantage of the random selection of candidate characteristics for the pre-selection of attributes in supervised classification.

1 Introduction

1.1 Context

For the oil company Total, the geological study of a potentially rich in hydrocarbons subsoil requires a thorough understanding of its structure.

To achieve that, the geologists create, from seismic images reconstructed by acoustic

Francois Meunier
Sorbonne Universités, Total EP, Paris
e-mail: Francois.Meunier@lip6.fr

Christophe Marsala
Sorbonne Universités, UPMC Univ Paris 06, CNRS, LIP6 UMR 7606
4 place Jussieu, 75005 Paris
e-mail: Christophe.Marsala@lip6.fr

Laurent Castanie
Total Exploration-Production, Tour Coupole, La Défense
2 Place Jean Millier, 92800 Puteaux
e-mail: Laurent.Castanie@total.com

waves sent into the ground (Fig. 1), a 3D geo-model that is supposed to represent the main layers and faults of the zone (Fig. 2). The geo-model, made of 3D surfaces corresponding to the boundaries between the sedimentary layers, only describes the geometrical structure of the subsoil.

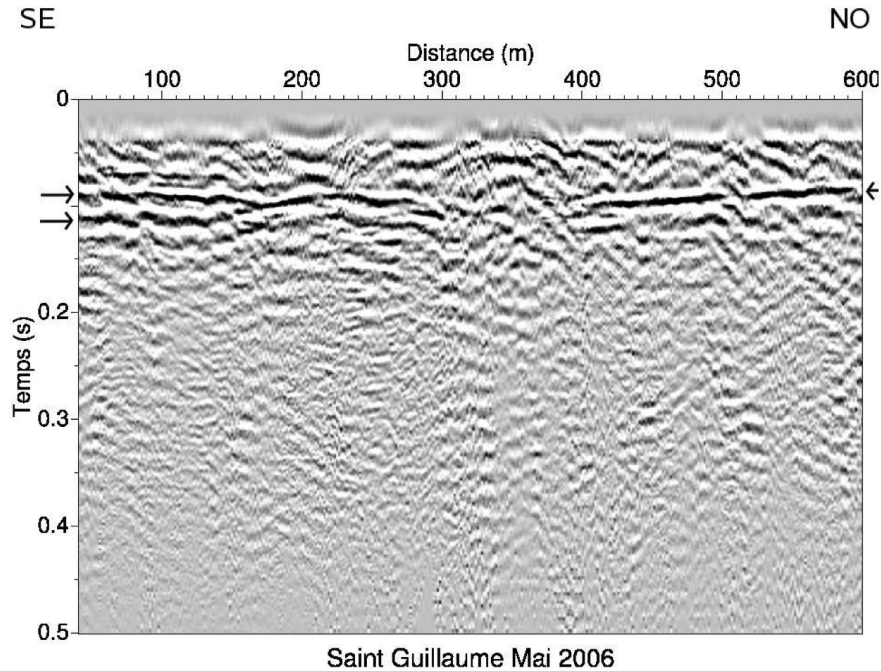


Fig. 1 Seismic image rebuilt using acoustic waves data

Then, this one is, according to the phenomena found there, classified by the geologist according to the relevant sets to which it belongs. The sets we talk about correspond to the presence or absence of a certain geological phenomenon, such as faults (normal, inverse, ...) or interaction between different layers (subduction, ...). For a geologist, it is therefore necessary to determine the absence or presence of local geological phenomena.

Today, this classification, like the rest of the study, is manually performed by an experienced geologist who knows the area. This represents a significant workload, which can be greatly facilitated by automation. Moreover, some geologists have less experience, both in the trade itself and the people most useful to contact, which results in a poor classification.

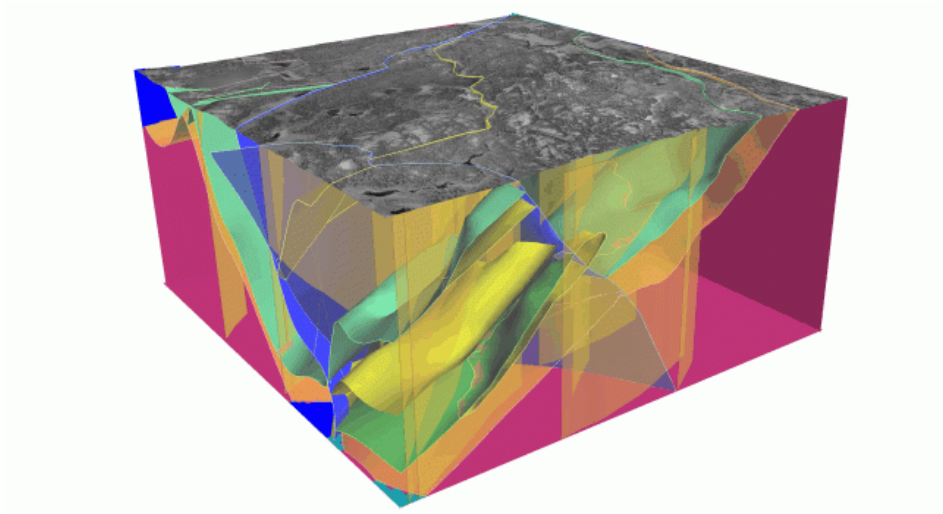


Fig. 2 3D geo-model of the studied zone

1.2 Our goals

Over the past few years, supervised automated learning has offered new possibilities to help classifying data of any type. Nevertheless, for 3D objects, current methods do not allow, without any prior knowledge, to understand which sub-parts of an object can be discriminating for the classification (describing the presence of the studied phenomenon), and why.

This problem is frequently back when automatic learning, for which the resolution is perceived from the the user's point of view as a "black box" whose confidence can be attributed to him only according to his past performances. The interest is therefore trying to explain the result of classification to the user, so that the user can actually validate the model and therefore the contribution of the latter.

The data to be categorized are complex by the number of points which compose them, and logically integrate large quantities of information, exploitable but little exploited.

The constraints of the system, and therefore the conditions of application of the proposed method are as follows:

- Learning elements are 3D surfaces of irregular triangular meshes;
- Classification is based on the presence of phenomena and/or sets of local phenomena;
- We place ourselves in traditional supervised learning, without any change in the distribution law of the classes in the studied set.

When processing complex elements, classifiers usually do not provide justification allowing to understand their processes and results. Within the framework of the supervised classification of 3D objects, the latter is very often carried out manually by industrialists, who are anxious to understand the reasons that pushed them to a particular choice for their studies.

This represents a significant workload, that automatizing the classification of these 3D objects would greatly facilitate, provided that they meet the constraints imposed by the manufacturers in terms of comprehensibility.

Our work proposes to set up a supervised classification system of 3D objects with explicit justification of the provided result.

Within this domain, current methods do not allow, without prior knowledge, to understand which sub-parts of an object could be discriminating in the context of the presence of the phenomenon studied, and why they would be.

In this article, after a state of the art presented in Section 2, the proposed method is described in Section 3, before Section 4 gives the experiments performed and Section 5 the perspectives of this method.

2 State of the art

With the existing methods of supervised classification of 3D objects, it is nowadays impossible to categorize 3D objects on the presence of local phenomena, while justifying the process and the predictions.

Methods derived from fields as varied as the processing of images or time series show unexploited possibilities in the extraction of discriminant sub-parts, using descriptors of 3D objects from the literature to characterize them.

The basic 3D model is a surface in a 3-dimensional space. We denote by $P \subseteq R^3$ the set of points on this surface. This is studied as a triangular mesh modeled as a graph $G = \{S, V, T\}$, with $S \subseteq P$ the vertices, $V = \{(s_1, s_2) \mid s_1, s_2 \in S\}$ the edges connecting the vertices and $T = \{(s_1, s_2, s_3) \mid s_1, s_2, s_3 \in S\}$ the triangles of the mesh. Subsequently, we consider the 3D model as a 3D surface such that $M = \{P, G\}$.

2.1 3D object descriptors

In the case of time series or images, it is possible to directly compare the data of the extracted sub-parts (with Euclidean distance, for example). For 3D objects, it is not possible to directly compare two entities of this same type because, in addition to having to establish an alignment according to translation, rotation, scale and reflection, it is essential to take into account that sampling does not necessarily

correspond from an extract to the other.

The computation of the minimum distance between each point of the first extract and the structure of the second is only possible in the presence of elements of the same extents. The study of 3D objects, described by non-regular meshes, therefore firstly requires to extract descriptors that are intended to convert the data into a workable form for learning and comparison. Approaches based on volume descriptors or object skeletons do not apply to non-closed surfaces [Alexandre, 2012].

There are currently many methods for extracting descriptors from 3D objects [Dang, 2014]. In addition to those that pass from 3D to 2D by cut or projection, which do not adapt to our problem because of the too great loss of data, distinction is generally done between local and global descriptors. The global descriptors are not adapted to our study, because over the whole structure they lose the purely local characteristics of the sub-parts that [Tabia, 2011] summarizes. Local descriptors can be good means for comparing different retrieved extracts as they are applied to small areas that potentially correspond to the discriminant sub-parts described in *Section 1*. Indeed, one considers only the tendencies in the neighborhood of a point of the mesh, which generally tends to use a histogram of distribution of values like [Dang, 2014] if we want to describe an entire surface as does [Ankerst et al., 1999] with the Shape Histogram, and [Rusu et al., 2008] with the *PFH* (Point Feature Histogram).

Although these two sets of global and local methods can differ to define a non-closed 3D surface, for our study, they must respect the following conditions:

- A good ability to represent a prototype of the concerned class (which is the local phenomenon detected);
- Robustness with respect to the main geometric transformations like scale or rotation;
- Being able to characterize a particular area within the 3D object;
- Being able to use it to justify the final classification.

2.2 Cloud scaling for pattern recognition

The aim is to find the best possible match between two clouds of different points in appearance, but which are described as close objects (or quite similar ones). It is done on sets of points, in order to recognize similar elements [Cotting et al., 2004].

Concretely, the principle of calibration can be seen [Mitra et al., 2004] as the search for the two transformations R and T from R^3 to R^3 (rotation and translation) between the clouds of points P and Q , minimizing the following relation:

$$\varepsilon(R, t) = \sum_{i=1}^{\|P\|} d^2(T((R(p_i))), \Phi_Q) \quad (1)$$

Where $d^2(T((R(p_i))), \Phi_Q)$ is the distance between the point $p_i \in P$ and Φ_Q (corresponding to the interpolation of the scatter of points to make it a surface) of the cloud Q . The classical way to solve this equation often amounts to calculating the distance between the transformed point $Rp_i + t$ and its closest neighbor p_i of the cloud Q , yet this function is not convex, and the *Iterative Closest Point* methods of [Besl and McKay, 1992] and *Random Sample Consensus* (or *RANSAC*) of [Fischler and Bolles, 1981] by gradient descent can only find a local solution (therefore approximated).

Moreover, the amount of exponentially increasing possibilities according to the number of points (notably by rotations, translations, ...) makes these methods hardly applicable to the detection of local phenomena.

Finally, this set of processes considers point clouds in an unsupervised way and thus can not distinguish what is to be retained from what is anecdotal within a particular supervised classification.

2.3 Distance / similarity between distribution histograms values

In order to compare two extracted sub-surfaces, the use of a local descriptor requires the use of a distance. The computation of the descriptor provides a set of data collected in a distribution histogram of values corresponding to each point of the surface retained. Several types of distances between histograms can then be used:

- the measure of [Bhattacharyya, 1943],
- the distance of [Matusita, 1955],
- the Hellinger measure,
- the divergence of [Kullback and Leibler, 1951].

2.4 Time series shapelets

Proposed by [Refregier, 2001], the notion of "shapelets" was initially applied to images. The method is based on a linear decomposition of each image into series of elementary functions describing local sub-parts: these functions are called "shapelets". Concretely, this makes it possible to obtain a simplified version of this data from complex data by decomposing them into entities which are easier to study.

This method was subsequently adapted to time series for supervised classification by [Ye and Keogh, 2009]. The principle is to extract the whole set of possible

sub-parts of each element of the learning set and then to determine which ones divide the best of all the elements, in order to maximize a particular indicator allowing to judge the capacity of discrimination.

The classical entropy maximization method retained by [Ye and Keogh, 2009] consists in computing the minimum distance between each candidate attribute and each object.

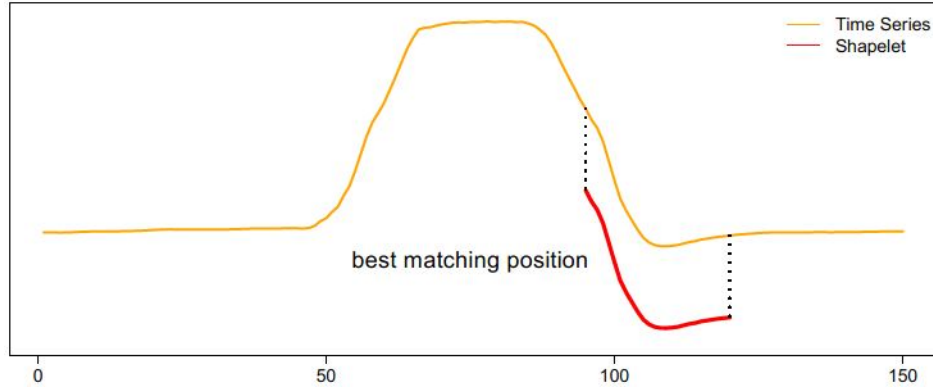


Fig. 3 The Time Serie Shapelets - [Ye and Keogh, 2009]

Then, for each candidate, we order the objects according to the distance separating them from this candidate.

Finally, we evaluate the discriminating capacity of the candidates, and the most efficient one when splitting the time series according to their classes are used to create the attributes of learning 4.

This indicator, resulting from the methods of *feature selection* of which [Chandrashekar and Sahin, 2014] studies the domain and [Renard et al., 2016] applies some methods to the time series, makes it possible to determine the most relevant of the sub-parts. This evaluation is carried out by the information gain which aims at measuring the dependence between 2 variables.

This information gain, or mutual information, is defined as follow:

Let Y be a discrete random variable, and $p(y)$ its probability (which corresponds to the proportion of elements of the class under consideration), we have the Shannon entropy:

$$H(Y) = - \sum_{y \in Y} p(y) \log(p(y)) \quad (2)$$

The conditional entropy of Y with X is defined by:

$$H(Y|X) = - \sum_{x \in X} \sum_{y \in Y} p(x, y) \quad (3)$$

The gain of information (Mutual Information or MI) of variable Y is finally valid:

$$I(Y, X) = H(Y) - H(Y|X) \quad (4)$$

This value is then used by testing each possible separation point between two sub-parts, and the point maximizing the gain is kept (Fig. 4).

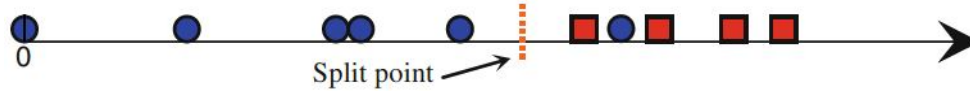


Fig. 4 Determining the most critical shapelets: ability to split all objects into 2 homogeneous sets - [Ye and Keogh, 2009]

In the ideal case, all the elements of a certain class are on the same side of the separation and are the only ones to be there.

[Lines et al., 2012] and [Hills et al., 2014] use the most discriminant shapelets by computing the minimum distance that best matches the new elements to assert, that is to say, the time series which are still not labeled.

Subsequently, these distances become the attributes used for learning and no longer the decision tree directly. It becomes possible to reduce the problem to conventional supervised learning, and thus to use other more efficient methods than the original decision trees. The obvious advantage of the shapelet method applied to time series is that it is possible to compare elements of very varied sizes and of which there is no *a priori* knowledge (as would be the elementary functions of the original method). It is no longer the elements in their entirety that can be useful, but the juxtaposition of some of the sub-parts of the latter, with different characteristics, which together make possible to deduce the classes of belonging.

In order to get some optimization in terms of computational time realized in this domain, [Renard et al., 2015] uses a random extraction of these sub-parts in the framework of the classification of time series. Due to the redundancy of discriminant sub-parts in the targeted data, classification performance remains very good.

2.5 Conclusion of the state of the art

Current methods dealing with 3D objects try to describe them by projecting into another representation space, often called a descriptor. These descriptors seek to simplify the initial objects by placing them on a model of representation that leads

to a significant loss of the quality of the data. This is all the more so since we are dealing with elements whose discriminating parts are extracted from them. The foreseeable result is that we are able to only consider some sub-parts of the object to classify it. The other blocking point is that it is impossible for the user, in this situation, to separate the useful parts from the other when trying to understand the method.

Thus, with the existing methods of supervised classification for 3D objects, it is not possible to categorize 3D objects on the presence of local phenomena, while justifying the process and the predictions.

Nevertheless, some work in the classification of time series has solved this problem by seeking to extract, for each classification, the most discriminating sub-parts.

Methods derived from fields as varied as the processing of images and time series present unexploited possibilities in the extraction of discriminating sub-parts, using descriptors of 3D objects of the literature allowing to characterize them.

It is on the basis of these concepts developed in the past years, where the random selection of potential features is one of the extensions, that we propose a new method answering the constraints cited above. This new approach is described in the next section, before experiments confirm its relevance.

3 Proposed method

3.1 Main idea

The proposed method for the classification of 3D objects is at the crossroads of the different domains presented in the previous section:

1. The shapelets, including the supervised classification of [Ye and Keogh, 2009] for time series;
2. The 3D surface similarity computations by extraction of 3D object descriptors.

These techniques appear to be potentially complementary. Indeed, the windowing of [Lozano Vega, 2015] of an image (in the form of a rectangle or a square extracted from this image) makes it possible to determine which part is the most interesting to be observed in the context of a particular classification. The initial idea of [Refregier, 2001] also makes it possible to test and extract the most discriminating sub-parts of a coherent set of data, within the desired classification.

Nevertheless, what is possible in the face of a mesh which can be drawn up as an exhaustive list of possible candidates, since it is rectangular in shape and in a set of predefined possible sizes, is problematic for irregular 3D meshes. Indeed, we are confronted to an explosion of the computation time for the extraction and evaluation of the very many candidates.

When [Renard et al., 2015] proposes a random search of potentially discriminating sub-parts for the classification of series Temporal, its results are hardly degraded. Indeed, due to large quantities of data, the redundancy of the discriminant extracts makes it possible not to decrease the performance of the prediction, when compared to the exhaustive model. This idea has been adapted to our problem, although in our case a much smaller share of the candidates as discriminant sub-part (the order of magnitude is about $10^{-1}\%$ for the time series of this work) has been retained.

Thus, we propose to adapt to 3D objects what has been done with the time series in classification, that is to say the selection of the discriminating sub-parts used to calculate the learning attributes being performed randomly by selecting only one extract of the set of possibilities.

3.2 Algorithm and methodology

- $\forall O_{i=1,\dots,n}$, we randomly extract m sub-surfaces (for each object O_i) that are $S_{i,1}, \dots, S_{i,m}$.
- We consider a particular 3D object descriptor $Desc$, and a distance $Dist$ (between to values of descriptors). $\forall i \in (1, \dots, n)$ and $\forall j \in (1, \dots, m)$, we compute the descriptor $Desc(S_{i,j})$, of the subsurface $S_{i,j}$

Then, for each sub-surface $S_{i,j}$ to evaluate:

- $\forall i' \in (1, \dots, n) \neq i$ and $\forall j' \in (1, \dots, m)$, we compute the proximity $Prox(S_{i,j}, S_{i',j'}) = Dist(Desc(S_{i,j}), Desc(S_{i',j'}))$.
- Degrees corresponding to its nesting values for each of the objects O_1, \dots, O_n is : $\forall i' \in (1, \dots, n)$.

$$Degree(S_{i,j}, O_{i'}) = \inf_{l=1,\dots,m} (Prox(S_{i,j}, S_{i',l}))$$

This matching degree or belonging degree of a subsurface to an object makes it possible to establish a form of proximity between the studied sub-surface and each object. It is on the basis of these values that the relevance score of each of the sub-surfaces is evaluated in order to select only the most discriminating ones. For the evaluation of the suitability of the subsurface from the degrees, and although [Ye and Keogh, 2009] uses the method of gaining information to evaluate still turns out that another method of *selection of attributes* is more adapted.

[Lines et al., 2012] proposes the use of the formula *f-stat*, more efficient for evaluating the discriminating character of a sub-part than the classical method. If we add a lower calculation time, this formula seems to be more appropriate.

For a subsurface $S_{i,j}$, in a C classes problem, we have:

$$f\text{-stat}(S_{i,j}) = \frac{\frac{1}{C-1} \sum_{cl=1}^C (\bar{D}_{cl} - \bar{D})^2}{\frac{1}{m-C} \sum_{cl=1}^C \sum_{d \in D_{cl}} (d - \bar{D}_{cl})^2} \quad (5)$$

with $C > 1$ the number of classes, m the number of sub-parts ($m > C$), \bar{D}_{cl} the average of the degrees between 3D objects of class cl and $S_{i,j}$, and \bar{D} the average of degrees between 3D objects of all classes and $S_{i,j}$.

Subsequently, the first k candidates according to this criterion will be used for the calculation of the attributes, k being experimentally around 1% of the total number of extracts.

It makes sense (and the results confirm) not to use more attributes than half of the number of sub-parts extracted from each 3D object. This can be explained fairly easily by the fact that if we put as many attribute sub-parts as extracts of a 3D object, then the attributes will lack choice in the selection of the closest extract when computing distance between object and candidate shapelet.

Once the most relevant sub-surfaces are extracted, they are used to carry out the learning on a traditional supervised classification model (the degrees between the element and each sub-surface gives the attribute vector), and, on the other hand, perform the same procedure for the prediction of new objects.

This results in Algorithm 1, called 3DRESC for *3D Random Extraction of Sub-parts for Classification*.

4 Experiments

The algorithm is adapted to a classification context of large 3D structures whose elements allowing the latter are only sub-parts, it is rather complicated to find a public dataset corresponding to our needs.

Indeed, the supervised classification of 3D objects generally answers the need for classifying closed objects, which belong as a whole to a class, whereas our objective was to detect local phenomena without knowing their shape or position within 3D structures.

Then, the choice of the computation of similarity between sub-parts (in order to calculate the distance between a candidate and a 3D object) is quite greedy in computation time. Still in the experimental state, it has not yet been optimized but this will be the subject of a future development.

Finally, and probably the essential point, our method aims at helping the user to understand the classification: the central element is therefore no longer the classifi-

Algorithm 1: 3DRESC

```

1 Input:
2 Objects : 3D objects ; Classes : corresponding classes ; k : number of expected attributes ;
   sizes : sizes of the extracts ; numbers : number of extracted sub-parts for each size ;
3 Output:
4 SubParts : List of discriminant 3D objects sub-parts;
5 Begin
6  $i \leftarrow 0$ ;
7 for Object in Objects do
8    $i \leftarrow i + 1$ ;
9    $j \leftarrow 0$ ;
10  candidates  $\leftarrow$  Extraction(Object, sizes, numbers);
11  for candidate in candidates do
12     $j \leftarrow j + 1$ ;
13    DescObject3D[i][j]  $\leftarrow$  ComputeDescriptor(candidate);
14 obj1  $\leftarrow 0$ ;
15 for Object1 in Objects do
16   obj1  $\leftarrow$  obj1 + 1;
17   obj2  $\leftarrow 0$ ;
18   for Object2 in Objects do
19    obj2  $\leftarrow$  obj2 + 1;
20    if Object1 different from Object2 then
21      Distances  $\leftarrow$   $\min$ (ComputeDistances(DescObject3D[obj1],
22      DescObject3D[obj2]));
23      Gain  $\leftarrow$  ComputeGain(Distances, Classes);
24      ListGain[i]  $\leftarrow$   $\max$ (Gain);
25 ListGain  $\leftarrow$  Ordonate(ListGain);
26 SubParts  $\leftarrow$  ListGain[1, ..., k];
27 End

```

cation itself (and therefore the prediction rate the ultimate objective), but the ability to provide an explanation for the given classification. We have tested our algorithm with free data from *Princeton Shape Benchmark*¹ (PSB), whose main advantage is to come from crawlers who have retrieved objects from multiple already existing datasets. The classifier used once the attributes are recovered is the random forests of the Python *scikit-learn* package. The tests are performed on a processor *Intel Core i7 vPro* with 16 GB of RAM. The sample comprises 40, 60 or 100 objects according to the experiment, divided into 2 classes of the same size. The objects themselves have very variable sizes, ranging from 250 points to about 5000 points. No standardization has been made, the small number of objects selected and the large standard deviation of objects' size (1946) logically reduces the results of the prediction.

Experiments carried out with descriptors of the literature are done under the same conditions as those used for the proposed method, namely the same libraries and the

¹ [http : //shape.cs.princeton.edu/benchmark/](http://shape.cs.princeton.edu/benchmark/) accessed 29/09/2016

same extraction of descriptors (depending on whether it is extracted from sub-parts or the object as a whole).

4.1 Choice of the descriptor and the computation of similarity

Starting from local descriptors, which give the local tendency around each point, we recover an histogram of values distribution. It is using this normalized histogram, whose size is constant whatever that of the original subsurface, that the distance is calculated. By extracting 200 sub-surfaces of size each time by cross-validation (by learning about 75% and testing on 25% at each iteration) on 60 objects (subdivided into 2 classes of the same sizes), the performances of the 3D object descriptors, that is to say the *Heat Kernel Signature* [Sun et al., 2009] (HKS), the *Point Feature Histogram* (PFH), and the *Unique Shape Context* (USC), are in Table 1.

3D object descriptor	Kullback-Leibler divergence	Bhattacharyya measure	Hellinger distance	Matusita distance	Computation time (seconds)
HKS	0.89 ± 0.13	0.85 ± 0.13	0.86 ± 0.07	0.90 ± 0.12	1208
PFH	0.79 ± 0.16	0.75 ± 0.14	0.60 ± 0.08	0.71 ± 0.12	1098
USC	0.86 ± 0.11	0.85 ± 0.15	0.84 ± 0.13	0.87 ± 0.11	1152

Table 1 Compared performances between 3D object descriptors

As columns of Table 1, we find the method used for calculating the distance between the sub-parts, as well as the calculation time, and in rows the descriptors from which these distances are calculated.

Moreover, it also mentions the standard deviation of the cross-validation realized. The slight differences in computation time only depend on the implementation of the descriptor algorithms, and the order of magnitude remains the same. Best results are those of the HKS, although the USC is following it. With the dataset that is ours, it appeared that Matusita’s distance, combined with this same HKS, seems to form the best combination.

For our future experiments, we therefore choose as 3D object descriptor the HKS and as distance between these descriptors, the distance of Matusita. It is nevertheless observed that any 3D object descriptor can be used to describe the extracted sub-surfaces, and thus that the true comparison must take place between a global descriptor and our method using the same descriptor for each of the extracted sub-parts.

4.2 The choice of the number of extracts

By reusing the *HKS* descriptor chosen previously, a learning set of 40 and 100 objects, 2 classes of the same size but randomly drawn from the *PSB*, results are given in Table 2.

Number of 3D objects	Number of extracted sub-parts (per object)	Classification rate	Computation time (seconds)
40	25	0.65 ± 0.15	122
	50	0.75 ± 0.16	237
	100	0.81 ± 0.14	468
	200	0.87 ± 0.10	831
	300	0.89 ± 0.11	1469
	400	0.92 ± 0.08	2160
	<i>HKS</i> global	0.85 ± 0.08	1020
100	25	0.59 ± 0.28	230
	50	0.71 ± 0.29	396
	100	0.78 ± 0.18	902
	200	0.87 ± 0.16	1728
	300	0.90 ± 0.14	2645
	400	0.91 ± 0.13	3587
	<i>HKS</i> global	0.82 ± 0.11	2285

Table 2 Compared performances : accuracy for 40 and 100 objects

The first column of Table 2 indicates the number of extracted sub-surfaces and their sizes.

For example, for the first line, 40 sub-surfaces were for each object extracted, with sizes of 20, 40, 60 and 80 points connected. As for the comparison between descriptors, the good classification rates of the 2nd column are completed by the standard deviation of the cross-validation. The last line presents the results of a global classification method using the histograms of the *HKS* of the set of points as attributes.

On the first hand, the more the extract sizes are varied, the more the number of these extracts increases, the better the classification. The confidence for the predictions is rather limited, this is due to the random selection of the sub-parts which makes the method slightly less stable than a deterministic one would be.

On the other hand, the proposed method is faster than the global one, since it only considers some of the parts of the object. What is more, the comparison can be reproduced with any descriptor, insofar as a way to define a 3D object can be adapted to our context.

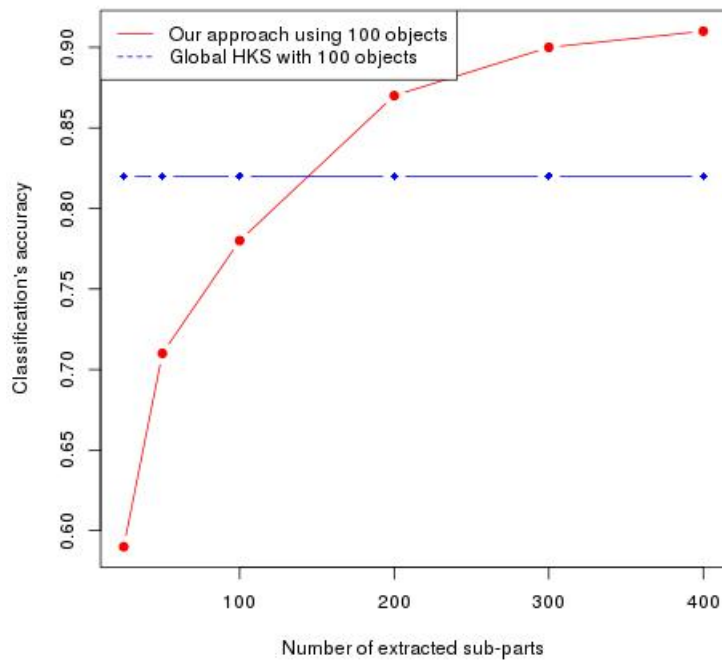
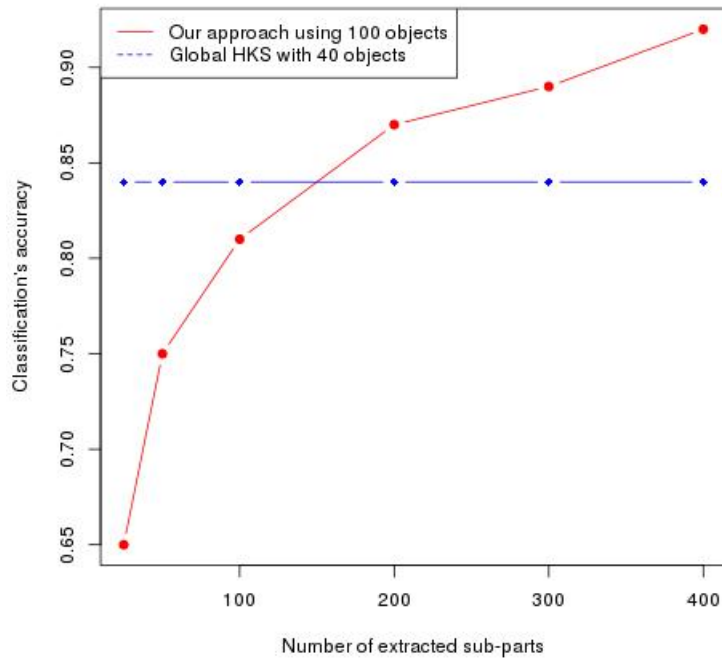


Fig. 5 Comparison of classification rate according to the number of extracts per object

4.3 Comparison with other methods of supervised classification for 3D objects

By way of indication, here is a comparison of the most used methods with our proposition, although these techniques don't allow the user to understand results and processes (Table 3).

This time, tests are performed with 60 objects from two classes of the same size of the *PSB*.

We chose to use 200 extracts per object, which was a good compromise between the execution time and the accuracy of the classification, if we refer to Fig. 5.

3D object classification method	Classification accuracy	Computation time (seconds)
Spherical harmonics	0.71 ± 0.09	1205
Shape Histogram [Ankerst et al., 1999]	0.74 ± 0.07	952
Extended Gaussian image [Horn, 1984]	0.83 ± 0.10	1452
Gaussian Euclidean Distance Transform [Kazhdan et al., 2003]	0.88 ± 0.08	1356
Hough 3D and SURF [Knopp et al., 2010]	0.87 ± 0.06	1325
Global USC	0.83 ± 0.08	1244
Global PFH	0.78 ± 0.10	1546
Global HKS	0.84 ± 0.07	1253
Our method	0.89 ± 0.12	1152

Table 3 Compared performances between 3D object classification methods with Princeton Shape Benchmark

We notice that our method gets results which are globally better than those from the literature, for a same order of magnitude computation time, although it is only a simple classification (2 classes) on a restricted number of 3D objects (60).

4.4 Interpretation of discriminant sub-parts

The principal contribution of our method, insofar as its results are a bit better than those from the literature, is to be able to make it possible to understand the proposed classification by the exhibition of the sub-parts that have been chosen for being the most relevant ones. In our example, it was a question of classifying 3D objects between 2 categories, which were on one hand inanimate objects, and on the other hand heads or busts of a human body.

The 2 first extracts such as those in Fig. 7 correspond to human anatomy (probably the curved part of the back of a head). The last one is the column of a building, something we can't find on a human body, and so is pertinent to discriminate these 2 classes.

These elements allow to display some of the sub-parts that have made it possible to create the attributes of the object and therefore the extracts which are the most

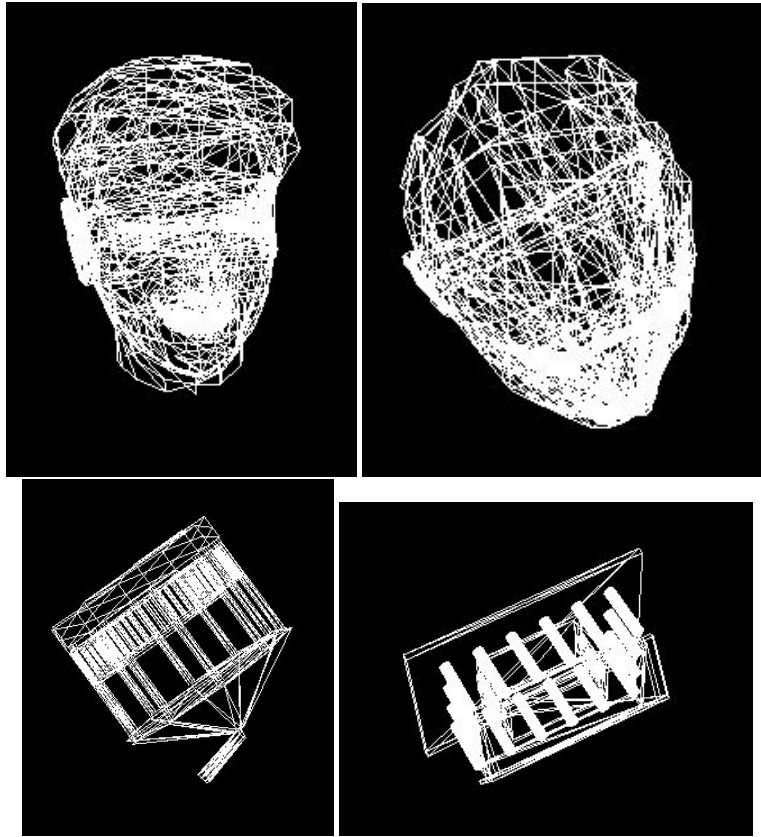


Fig. 6 3D objects to classify : the first one are from the visages' class, and the rest from the building's

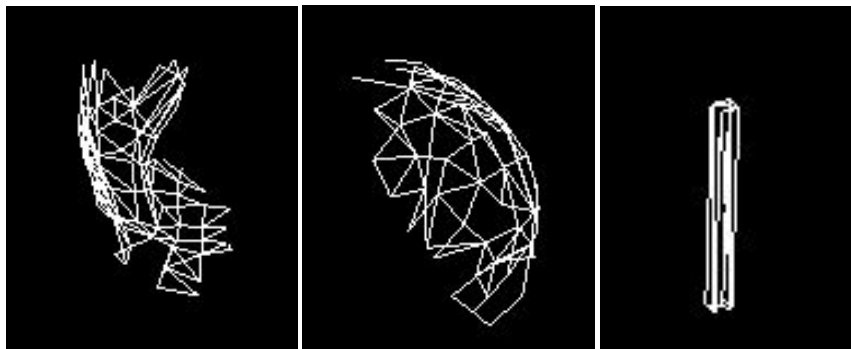


Fig. 7 3D objects discriminant sub-parts : the 2 first ones are curves of a head, the last one is the column of a building

representative of the classification. By this mean, we expect to convince the experts that the choice of the classifier is justified, and so that this classifier may be used for their work.

5 Conclusion and perspectives

In this paper, we proposed a new method for classifying 3D objects with a justification of the method and results by exhibiting the most discriminating elements.

Although the classification rate results for comparing to other techniques only correspond to a part of the true objective of this algorithm (to show the user discriminating sub-parts to help him to understand the classification).

However, the proposition we do is at least as good (in fact slightly better) than the more traditional methods, although the randomness seems to slightly decrease the stability.

The first visualization experiments are promising, but require confirmation of a pre-production in the targeted trade in order to meet the needs of geologists.

Moreover, some choices of parameters of the algorithm, that is to say the number of sub-parts per object, the size of these sub-parts, the number of sub-parts selected for learning, have been chosen only by successive empirical tests on different data sets, and by giving our confidence to previous publications.

In the end, we will of course try to automate these choice of parameters.

Continuing on this axis of research involves questioning the set of values given to the parameters. Indeed, the real data the algorithm is going to be confronted to will tend to make reconsider some decisions that can be arbitrary, such as the choice of the size of the extracted sub-parts (applied to the problem) and their number. This could be the initial knowledge required for the classification, although automatizing is possible in the medium term.

By the crossing of the techniques used for time series and image processing, our method aims at helping an expert to better understand the key areas of a 3D object in order to understand the set studied.

In addition to this direct application, we can easily see the possibility of reusing the method proposed in this article for the automated processing of point clouds to help, for example, a robot recognizing objects.

Moreover, in order to adapt this model to more common situations of classification of 3D structures, trying to adapt it to cases of partially "hidden" objects would be appropriate too, thus allowing to also use it in computer vision.

References

- [Alexandre, 2012] Alexandre, L. A. (2012). 3D Descriptors for Object and Category Recognition: a Comparative Evaluation. In *Workshop on Color-Depth Camera Fusion in Robotics at the IEEE/RSJ International Conference on Intelligent Robots and Systems (IROS)*, Vilamoura, Portugal.
- [Ankerst et al., 1999] Ankerst, M., Kastenmüller, G., Kriegel, H.-P., and Seidl, T. (1999). 3d shape histograms for similarity search and classification in spatial databases. In *Proceedings of the 6th International Symposium on Advances in Spatial Databases, SSD '99*, pages 207–226, London, UK. Springer-Verlag.
- [Besl and McKay, 1992] Besl, P. J. and McKay, N. D. (1992). A method for registration of 3-d shapes. *IEEE Trans. Pattern Anal. Mach. Intell.*, 14(2):239–256.
- [Bhattacharyya, 1943] Bhattacharyya, A. (1943). On a measure of divergence between two statistical populations defined by their probability distributions. *Bulletin of Cal. Math. Soc.*, 35(1):99–109.
- [Chandrashekar and Sahin, 2014] Chandrashekar, G. and Sahin, F. (2014). A survey on feature selection methods. *Computers and Electrical Engineering*, pages 16–28.
- [Cotting et al., 2004] Cotting, D., Weyrich, T., Pauly, M., and Gross, M. H. (2004). Robust watermarking of point-sampled geometry. In *SMI*, pages 233–242. IEEE Computer Society.
- [Dang, 2014] Dang, Q. V. (2014). *Similarités dans des modèles BRep paramétriques: detection et applications*. PhD thesis, Université de Toulouse.
- [Fischler and Bolles, 1981] Fischler, M. A. and Bolles, R. C. (1981). Random sample consensus: A paradigm for model fitting with applications to image analysis and automated cartography. *Commun. ACM*, 24(6):381–395.
- [Hills et al., 2014] Hills, J., Lines, J., Baranauskas, E., Mapp, J., and Bagnall, A. (2014). Classification of time series by shapelet transformation. *Data Min. Knowl. Discov.*, 28(4):851–881.
- [Horn, 1984] Horn, B. K. P. (1984). Extended gaussian images. *Proceedings of the IEEE*, 72(2):1671–1686.
- [Kazhdan et al., 2003] Kazhdan, M., Funkhouser, T., and Rusinkiewicz, S. (2003). Rotation invariant spherical harmonic representation of 3d shape descriptors. In *Proceedings of the 2003 Eurographics/ACM SIGGRAPH Symposium on Geometry Processing, SGP '03*, pages 156–164, Aire-la-Ville, Switzerland, Switzerland. Eurographics Association.
- [Knopp et al., 2010] Knopp, J., Prasad, M., Willems, G., Timofte, R., and Gool, L. J. V. (2010). Hough transform and 3d surf for robust three dimensional classification. In Daniilidis, K., Maragos, P., and Paragios, N., editors, *ECCV (6)*, volume 6316 of *Lecture Notes in Computer Science*, pages 589–602. Springer.
- [Kullback and Leibler, 1951] Kullback, S. and Leibler, R. A. (1951). On information and sufficiency. *The Annals of Mathematical Statistics*, 22(1):79–86.
- [Lines et al., 2012] Lines, J., Davis, L. M., Hills, J., and Bagnall, A. (2012). *A Shapelet Transform for Time Series Classification*. KDD '12. ACM, New York, NY, USA.
- [Lozano Vega, 2015] Lozano Vega, G. (2015). *Image-based detection and classification of allergenic pollen*. Theses, Université de Bourgogne.
- [Matusita, 1955] Matusita, K. (1955). Decision rules, based on the distance, for problems of fit, two samples, and estimation. *Annals of Mathematical Statistics*, 26(4):631–640.
- [Mitra et al., 2004] Mitra, N. J., Gelfand, N., Pottmann, H., and Guibas, L. (2004). Registration of point cloud data from a geometric optimization perspective. In *Symposium on Geometry Processing*, pages 23–31.
- [Refregier, 2001] Refregier, A. (2001). Shapelets: I. a method for image analysis. *Mon. Not. Roy. Astron. Soc.*, 338:35.
- [Renard et al., 2015] Renard, X., Rifqi, M., and Detyniecki, M. (2015). Random-shapelet: an algorithm for fast shapelet discovery. In *Proceedings of the IEEE International Conference on Data Science and Advanced Analytics (DSAA'2015)*, pages 1–10.
- [Renard et al., 2016] Renard, X., Rifqi, M., Fricout, G., and Detyniecki, M. (2016). EAST representation: fast discovery of discriminant temporal patterns from time series. In *ECML/PKDD Workshop on Advanced Analytics and Learning on Temporal Data*, Riva Del Garda, Italy.

- [Rusu et al., 2008] Rusu, R. B., Blodow, N., Marton, Z. C., and Beetz, M. (2008). Aligning Point Cloud Views using Persistent Feature Histograms. In *Proceedings of the 21st IEEE/RSJ International Conference on Intelligent Robots and Systems (IROS), Nice, France, September 22-26*.
- [Sun et al., 2009] Sun, J., Ovsjanikov, M., and Guibas, L. (2009). A Concise and Provably Informative Multi-scale Signature Based on Heat Diffusion. pages 1383–1392.
- [Tabia, 2011] Tabia, H. (2011). *Contributions to 3D-shape matching retrieval and classification*. PhD thesis, Université Lille 1.
- [Ye and Keogh, 2009] Ye, L. and Keogh, E. (2009). Time Series Shapelets: A New Primitive for Data Mining. In *Proceedings of the 15th ACM SIGKDD International Conference on Knowledge Discovery and Data Mining, KDD '09*, pages 947–956, New York, NY, USA. ACM.